

# Pure-Gas and Vapor Permeation and Sorption Properties of Poly[1-phenyl-2-[*p*-(trimethylsilyl)phenyl]acetylene] (PTMSDPA)

L. G. Toy, K. Nagai, and B. D. Freeman\*

North Carolina State University, Department of Chemical Engineering, Box 7265,  
Raleigh, North Carolina 27695-7265

I. Pinnau\* and Z. He

Membrane Technology and Research, Inc., 1360 Willow Road, Suite 103,  
Menlo Park, California 94025-1516

T. Masuda and M. Teraguchi

Kyoto University, Department of Polymer Chemistry, Kyoto 606-8501, Japan

Yu. P. Yampolskii

Institute of Petrochemical Synthesis, Russian Academy of Sciences, 29 Leninsky Prospekt,  
117912, Moscow, Russia

Received September 14, 1999; Revised Manuscript Received January 24, 2000

**ABSTRACT:** The pure-gas permeation and sorption properties of poly[1-phenyl-2-[*p*-(trimethylsilyl)phenyl]acetylene] [PTMSDPA] are presented and compared to those of poly(1-trimethylsilyl-1-propyne) [PTMSP], poly(4-methyl-2-pentyne) [PMP], and poly(1-phenyl-1-propyne) [PPP]. PTMSDPA is more permeable to large, condensable vapors (e.g., *n*-butane) than to small, permanent gases (e.g., hydrogen). Such behavior is also observed in PTMSP and PMP but not in PPP. PTMSDPA has lower fractional free volume (0.26) and gas permeabilities than PTMSP and PMP. However, relative to conventional glassy polymers, PTMSDPA is a highly permeable, high free volume, glassy material. For example, the oxygen permeability coefficient of PTMSDPA is  $1200 \times 10^{-10} \text{ cm}^3(\text{STP}) \cdot \text{cm}/(\text{cm}^2 \cdot \text{s} \cdot \text{cmHg})$  at 25 °C. As temperature increases, the permeability in PTMSDPA increases for light gases (helium, hydrogen, and nitrogen) and decreases for more condensable gases. In contrast, the permeabilities of PTMSP and PMP decrease with increasing temperature for both light gases and more condensable hydrocarbons. *n*-Butane and propane sorption isotherms for PTMSDPA are concave to the penetrant relative pressure axis, consistent with dual-mode sorption behavior. Hydrocarbon sorption levels decrease in the order PTMSP > PMP > PTMSDPA > PPP, in agreement with the ranking of the fractional free volumes of the materials.

## Introduction

Certain glassy, disubstituted, acetylene-based polymers have high vapor permeability and high vapor selectivity for gas/vapor separations.<sup>1–4</sup> These very rigid, amorphous polymers contain alternating double bonds along the chain backbone and bulky side groups that hinder chain segmental motion and frustrate packing of polymer chains in the solid state. They are characterized by high glass transition temperatures (typically >200 °C), high fractional free volumes, and high gas permeabilities. Attracting the most attention within this family of materials is poly(1-trimethylsilyl-1-propyne) [PTMSP], which has a high fractional free volume (0.29) and the highest gas permeabilities of all known polymers.<sup>5,6</sup> These extremely high gas permeabilities result from very high gas solubility<sup>7</sup> and diffusivity coefficients,<sup>6</sup> which presumably derive in part from a very open polymer matrix and, for diffusivity, interconnectivity of the free volume elements.<sup>2,3,8</sup> Such a structure of interconnected, microporous domains provides very efficient pathways for gas permeation in PTMSP.

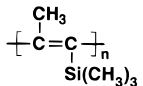
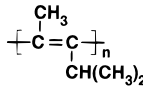
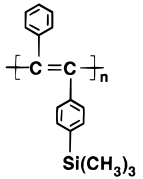
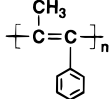
For permanent-gas separations, the high permeabilities of PTMSP are coupled with very low selectivities.<sup>1,3,6</sup> However, for the separation of condensable, organic vapors from permanent gases (i.e., gases with critical

temperatures significantly below room temperature), PTMSP is more permeable to organic vapors than to permanent gases and possesses very high vapor/gas selectivities, particularly under mixture conditions. For hydrocarbon vapor separations, PTMSP exhibits the highest mixture C<sub>3+</sub>/CH<sub>4</sub> and C<sub>3+</sub>/H<sub>2</sub> selectivities combined with the highest mixture C<sub>3+</sub> permeabilities of all known polymers.<sup>1–3</sup> A structurally similar, disubstituted acetylene polymer, poly(4-methyl-2-pentyne) [PMP], is also vapor-selective.<sup>9</sup> Synthesized more than a decade ago by Masuda et al.,<sup>10</sup> glassy PMP has a fractional free volume of 0.28 and is the most permeable, hydrocarbon-based polymer known.<sup>9</sup> To illustrate the broad range of permeation properties encompassed within this family of substituted acetylene polymers, poly(1-phenyl-1-propyne) [PPP] has a relatively high fractional free volume of 0.22 but is among the least permeable of these polymers.<sup>11–14</sup> In fact, like conventional glassy polymers, PPP is more permeable to small gases (e.g., hydrogen) than to large vapors (e.g., *n*-butane).<sup>14</sup>

While the permeation properties of many disubstituted acetylene polymers to light gases (i.e., permanent gases) have been reported,<sup>11–13,15</sup> much less data on the vapor permeation properties of this interesting class of polymers are available. Poly[1-phenyl-2-[*p*-(trimethylsilyl)phenyl]acetylene] [PTMSDPA] is a *para*-substitut-

\* To whom correspondence should be addressed.

**Table 1. Physical Properties of Glassy, Disubstituted Acetylene Polymers**

polymer	chemical repeat unit	density (g/cm <sup>3</sup> )	fractional free volume (FFV) <sup>a</sup>
PTMSP		0.75 <sup>b</sup>	0.29
PMP		0.78 <sup>c</sup>	0.28 <sup>c</sup>
PTMSDPA		0.91	0.26
PPP		1.0 <sup>d</sup>	0.22 <sup>e</sup>

<sup>a</sup> Calculated using eq 4, where occupied volume  $v_0 \approx 1.3v_W$  was estimated from group contribution methods.<sup>23</sup> <sup>b</sup> Reference 19. <sup>c</sup> Reference 9. <sup>d</sup> References 14 and 20. <sup>e</sup> Reference 14.

ed poly(diphenylacetylene) and, like PTMSP and PMP, is highly permeable.<sup>15–17</sup> In this paper, pure-gas permeabilities and pure hydrocarbon solubilities of PTMSDPA are presented and compared to those of PTMSP, PMP, and PPP. This is the first report of the hydrocarbon vapor permeation and sorption properties of PTMSDPA as well as the first account of the hydrocarbon vapor sorption properties of PMP. Additionally, the temperature dependence of gas permeability coefficients in PTMSDPA is presented and compared to available data on PTMSP, PMP, and a conventional glassy polyimide.

## Experimental Section

**Acetylene Polymer Film Preparation and Characterization.** PTMSDPA was synthesized with a TaCl<sub>5</sub>-*n*-Bu<sub>4</sub>Sn catalyst system as suggested by Tsuchihara et al.<sup>16,17</sup> and used as received. PMP was synthesized with a NbCl<sub>5</sub>-Ph<sub>3</sub>Bi catalyst system as described by Morisato and Pinnau.<sup>9</sup> The chemical structures and some physical properties of PTMSDPA and PMP are compared to those of PTMSP and PPP in Table 1.

Isotropic, dense films of PTMSDPA and PMP were prepared by casting a polymer solution into a flat-bottomed glass dish or a glass ring supported by a glass plate at ambient conditions. The films were cast from solutions of 1 wt % PTMSDPA in toluene and 2 wt % PMP in carbon tetrachloride. The cast films were dried gradually at ambient conditions for 2–3 weeks. Following this initial solvent evaporation step, the films were removed from the glass dish or plate by immersion in water and placed overnight in a vacuum oven at 70–80 °C to remove residual solvent. Film thickness was determined with a digital micrometer readable to  $\pm 1 \mu\text{m}$ . Final film thicknesses were 34–50  $\mu\text{m}$  for gas permeation measurements and 73–230  $\mu\text{m}$  for gas sorption studies. Film density was estimated by a gravimetric method. Several film samples were weighed on an analytical balance, and the density was calculated from the known sample area and film thickness.

**Gas Permeation Measurements.** The permeability of isotropic PTMSDPA films to permanent gases and hydrocarbons was measured using the continuous-flow, constant-pressure/variable-volume method.<sup>18</sup> The typical order of gas measurement used in the permeation experiments was nitrogen, oxygen, helium, hydrogen, methane, carbon dioxide,

ethane, propane, and *n*-butane. The feed pressure was 50 psig (4.4 atm, 446 kPa) for the permanent gases, methane, ethane, and propane and 8 psig (1.54 atm, 156 kPa) for *n*-butane; the permeate pressure was maintained at 0 psig (1.0 atm, 101 kPa). The experimental temperature was varied from 1.5 to 50 °C. The permeate gas flow rate was measured with a soap bubble flowmeter. The steady-state permeate flux  $J$  [cm<sup>3</sup>(STP)/(cm<sup>2</sup>·s)] was calculated from

$$J = \left( \frac{dV/dt}{A} \right) \left( \frac{273.15}{T} \right) \left( \frac{p_a}{76} \right) \quad (1)$$

where  $(dV/dt)$  is the steady-state, volumetric displacement rate (cm<sup>3</sup>/s) of soap film in the flowmeter,  $A$  is membrane area (cm<sup>2</sup>),  $T$  is temperature (K), and  $p_a$  is atmospheric pressure (cmHg). The gas permeability coefficient  $P$  [cm<sup>3</sup>(STP)·cm/(cm<sup>2</sup>·s·cmHg)] was computed from

$$P = \frac{J/l}{\Delta p} = \frac{J/l}{p_2 - p_1} \quad (2)$$

where  $l$  is the membrane film thickness (cm) and  $p_2$  and  $p_1$  are the feed and permeate pressures (cmHg), respectively. The selectivity  $\alpha_{A/B}$  of the polymeric films for component A over B was obtained from the ratio of pure gas permeabilities:

$$\alpha_{A/B} = \frac{P_A}{P_B} \quad (3)$$

**Gas Sorption Measurements.** The equilibrium uptake of pure propane and *n*-butane in PTMSDPA and PMP films was measured in interval, gravimetric sorption experiments conducted using an electrobalance system (model C-2000, Cahn Instruments, Inc., Madison, WI) at 35 °C. Contained in a thermoregulated, constant-temperature enclosure, this system consists of an electrobalance encased in a glass chamber connected to a vacuum line for sample degassing and penetrant removal. A uniformly thick polymer film sample was hung from one end of the balance beam of the electrobalance; appropriate counterweights were suspended from the other end. The entire sorption system was evacuated for at least 24 h to remove air and degas the polymer film. Hydrocarbon vapor was then introduced into the sorption chamber. The time-dependent change in polymer mass due to penetrant uptake at a fixed pressure was recorded electrically by a strip chart recorder connected to the electrobalance control unit. Penetrant uptake into the polymer film was allowed to reach equilibrium, which is characterized by a constant sample weight over a period of several hours. Incremental amounts of penetrant were then added to the sorption chamber to obtain subsequent data points. From the resulting data, the sorption isotherm for the polymer film was generated as a function of penetrant relative pressure  $a$ , which is defined as  $(p/p_{\text{sat}})$ , the ratio of the penetrant pressure  $p$  to the penetrant saturation vapor pressure  $p_{\text{sat}}$  at the experimental temperature. For an ideal gas, the relative pressure is equal to the thermodynamic activity of the gas. Penetrant relative pressures ranged up to about 0.08 (743 mmHg) for propane and 0.3 (736 mmHg) for *n*-butane.

## Results and Discussion

**Density and Fractional Free Volume of PTMSDPA.** As shown in Table 1, the chemical structure of PTMSDPA differs from that of PTMSP, PMP, and PPP only in the bulky substituents attached to the chain backbone. PTMSDPA has a phenyl group on the  $\alpha$ -carbon, while PTMSP, PMP, and PPP have a methyl group. On the second main-chain carbon, *para*-substituted PTMSDPA has a bulky (trimethylsilyl)phenyl [TMSPh] side-group, compared to PTMSP, PMP, and PPP which have a trimethylsilyl [TMS], an isopropyl, and a phenyl pendant group, respectively. The steric

bulkiness of these large substituents inhibits efficient, dense chain packing, leading to unusually high free volume in these polymers. This high free volume is coupled with a very low polymer density in PTMSP and PMP, which have densities of 0.75 and 0.78 g/cm<sup>3</sup>, respectively.<sup>9,19</sup> In contrast, the density of PPP is 1.0 g/cm<sup>3</sup>,<sup>14,20</sup> higher than that of PTMSP and PMP by ~30%. The density of the PTMSDPA films used in this study was 0.91 ± 0.02 g/cm<sup>3</sup>.

The fractional free volume (FFV) [cm<sup>3</sup> of free volume/cm<sup>3</sup> of polymer] is commonly used to characterize the efficiency of chain packing and the amount of space (free volume) available for gas permeation in a polymer matrix.<sup>21,22</sup> It is defined as<sup>21–23</sup>

$$\text{FFV} = \frac{v_{\text{sp}} - v_0}{v_{\text{sp}}} \approx \frac{v_{\text{sp}} - 1.3v_{\text{W}}}{v_{\text{sp}}} \quad (4)$$

where  $v_{\text{sp}}$  is the specific volume of the polymer and  $v_0$  is the occupied volume (or zero-point volume at 0 K) of the polymer. Typically, the occupied volume is estimated to be 1.3 times the van der Waals volume ( $v_{\text{W}}$ ), which is calculated from group contribution methods.<sup>21–24</sup> The factor of 1.3 is a universal packing parameter introduced by Bondi.<sup>24</sup>

The density-based FFV value estimated from eq 4 for PTMSDPA is compared to the FFV values of PTMSP, PMP, and PPP in Table 1. Of these four substituted acetylene polymers, PPP has the lowest FFV (~0.22), and PTMSP has the highest FFV (~0.29). The FFV of PMP is almost as high as that of PTMSP. For comparison, conventional glassy polymers (e.g., polysulfone, polyimide) have much lower fractional free volumes. The FFV values of such conventional glassy polymers typically vary from 0.11 to 0.22.<sup>21</sup> Thus, unlike PPP, whose FFV value is near the high end of the FFV range for common glasses, PTMSDPA, like PTMSP and PMP, falls into the category of ultrahigh free volume polymers.

Disubstituted acetylene polymers are also extremely stiff materials due to a combination of bulky substituents and the alternating double-bond structure in the chain backbone. Consequently, these materials have high glass transition or softening temperatures. On the basis of dynamic viscoelastic measurements, the glass transition temperature is estimated to be greater than 250 °C for PTMSP,<sup>25</sup> about 200 °C for PPP,<sup>13</sup> and greater than 200 °C for PTMSDPA.<sup>16,17</sup> PMP has a softening temperature of about 250 °C.<sup>9</sup> Because all gas permeation and sorption data were obtained at temperatures much lower than 200 °C, the substituted acetylene polymers discussed in this paper were studied in their glassy state.

**Gas Permeation Properties of PTMSDPA.** The small 7–10% reduction in the FFV value of PTMSDPA, relative to that of PTMSP and PMP, is accompanied by a substantial permeability decrease, as shown in Table 2. Compared to the permeabilities of PTMSP, the nitrogen permeability of PTMSDPA is reduced by a factor of 11, and its hydrocarbon vapor permeabilities are 5–10 times lower. On the basis of the data in this table and in Figure 1, the general pure-gas permeability ranking of the four disubstituted acetylene polymers is PTMSP > PMP > PTMSDPA > PPP. The gas permeability is often correlated with the fractional free volume in an amorphous polymer through the expression<sup>22</sup>

**Table 2.** Gas Permeabilities of PTMSP, PMP, PTMSDPA, and PPP at 25 °C

gas	critical temp (T) <sup>a</sup> (K)	permeability (barrer) <sup>f</sup>			
		PTMSP <sup>b,d</sup>	PMP <sup>c,d</sup>	PTMSDPA	PPP <sup>e</sup>
He	5.19	6500	2600	1100	
H <sub>2</sub>	33.2	17000	5800	2600	280
N <sub>2</sub>	126.2	6300	1300	560	21
O <sub>2</sub>	154.6	9700	2700	1200	57
CH <sub>4</sub>	190.4	15000	2900	1600	
CO <sub>2</sub>	304.1	34000	11000	4900	260
C <sub>2</sub> H <sub>6</sub>	305.4	26000	3700	2700	
C <sub>3</sub> H <sub>8</sub>	369.8	32000	7300	4400	
<i>n</i> -C <sub>4</sub> H <sub>10</sub>	425.2	102000	26000	20000	52

<sup>a</sup> Reference 38. <sup>b</sup> Reference 3. <sup>c</sup> Reference 9. <sup>d</sup> C<sub>3</sub>H<sub>8</sub> and *n*-C<sub>4</sub>H<sub>10</sub> permeabilities in refs 3 and 9 are somewhat different from the values reported here because they are reported at different feed pressures/temperatures than those used in this study. <sup>e</sup> Reference 14. <sup>f</sup> 1 barrer = 10<sup>-10</sup> cm<sup>3</sup>(STP)·cm/(cm<sup>2</sup>·s·cmHg). Feed pressure = 50 psig (446 kPa), except for *n*-C<sub>4</sub>H<sub>10</sub> (8 psig (156 kPa) for PTMSP, PMP, and PTMSDPA; 16 psig (212 kPa) for PPP). Permeate pressure = 0 psig (101 kPa).

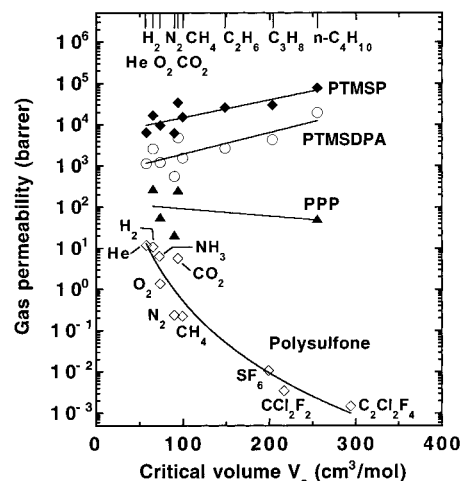


**Figure 1.** Comparison of gas permeabilities in PTMSDPA (○) to permeabilities reported for PTMSP<sup>3</sup> (◆), PPP<sup>14</sup> (▲), and low free volume, glassy polysulfone<sup>26</sup> (◇) as a function of penetrant critical volume (size)<sup>38</sup> at 25 °C. [1 barrer = 10<sup>-10</sup> cm<sup>3</sup>(STP)·cm/(cm<sup>2</sup>·s·cmHg).]

$$P = A \exp\left(-\frac{B}{\text{FFV}}\right) \quad (5)$$

where  $A$  and  $B$  are adjustable constants. Figure 2 shows that the oxygen permeability data for the four acetylene polymers are in good agreement with eq 5. As the FFV diminishes from 0.29 to 0.22, oxygen permeability decreases by roughly 2 orders of magnitude. Similar results are obtained for the other gases.

As demonstrated in Table 2 and Figure 1, for the series of C<sub>1</sub>–C<sub>4</sub> alkanes, hydrocarbon permeabilities in PTMSDPA increase with increasing critical temperature (i.e., condensability) and critical volume (i.e., size) of the penetrants. In fact, its propane and *n*-butane permeabilities are even higher than those of hydrogen and helium, the smallest penetrants investigated. Therefore, like PTMSP and PMP, high free volume, glassy PTMSDPA preferentially permeates larger, more condensable vapor molecules over smaller, less condensable, permanent-gas molecules. This vapor-selective behavior is in contrast to the permeation behavior observed for PPP and common, low free volume, glassy materials (e.g., polysulfone). For example, Table 2 shows that the permeability of PPP is significantly lower to



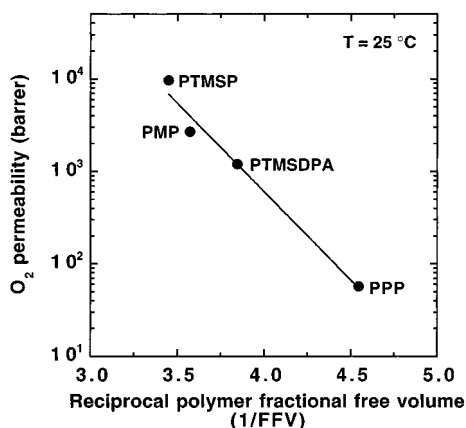


**Figure 2.** Correlation of oxygen ( $\text{O}_2$ ) permeability in four disubstituted acetylene polymers (PTMSP,<sup>3</sup> PMP,<sup>9</sup> PTMSDPA, and PPP<sup>14</sup>) with reciprocal fractional free volume ( $1/\text{FFV}$ ) of the polymer. FFV was calculated using group contribution methods according to eq 4.<sup>23</sup> [1 barrer =  $10^{-10} \text{ cm}^3(\text{STP})\cdot\text{cm}/(\text{cm}^2\cdot\text{s}\cdot\text{cmHg})$ .]

**Table 3.** Selectivities of Various Gases over Nitrogen in PTMSP, PMP, PTMSDPA, and PPP at 25 °C

gas	gas/ $\text{N}_2$ selectivity			
	PTMSP <sup>a</sup>	PMP <sup>b</sup>	PTMSDPA	PPP <sup>d</sup>
He	1.0	2.0	2.0	
$\text{H}_2$	2.7	4.5	4.6	13
$\text{O}_2$	1.5	2.1	2.1	2.7
$\text{CO}_2$	5.4	8.5	8.8	12
$\text{CH}_4$	2.4	2.2	2.9	
$\text{C}_2\text{H}_6$	4.1	2.8	4.8	
$\text{C}_3\text{H}_8$	5.1 <sup>c</sup>	5.6 <sup>c</sup>	7.9	
$n\text{-C}_4\text{H}_{10}$	16 <sup>c</sup>	20 <sup>c</sup>	36	2.5

<sup>a</sup> Reference 3. <sup>b</sup> Reference 9. <sup>c</sup> On the basis of unpublished  $\text{C}_3\text{H}_8$  and  $n\text{-C}_4\text{H}_{10}$  permeability data (see note in Table 2). <sup>d</sup> Reference 14.

$n$ -butane than to hydrogen. Figure 1 shows that this decrease in permeability with increasing penetrant size is much stronger for polysulfone,<sup>26</sup> a conventional glassy polymer used for gas separation, than for PPP, in qualitative agreement with predictions from free volume theory.<sup>27</sup> PTMSDPA permeability coefficients are also orders of magnitude higher than those of polysulfone and other common glasses.<sup>21,26</sup> The high gas permeabilities and vapor-selective nature of PTMSDPA, like those of PTMSP and PMP, are ascribed to its uncommonly large FFV.<sup>3,9</sup> However, the distribution of free volume in the polymer matrix may also play a key role in determining the gas transport properties in this family of high free volume, glassy disubstituted acetylene polymers.<sup>27</sup>

The pure-gas selectivities of PTMSDPA for various gases over nitrogen are summarized in Table 3 and compared to the selectivities of PTMSP, PMP, and PPP. In particular, the hydrocarbon/nitrogen selectivities of PTMSDPA, like those in PTMSP and PMP, increase as hydrocarbon condensability and size increase. PTMSDPA has selectivities of 2.9 for  $\text{CH}_4/\text{N}_2$ , 4.8 for  $\text{C}_2\text{H}_6/\text{N}_2$ , 7.9 for  $\text{C}_3\text{H}_8/\text{N}_2$ , and 36 for  $n\text{-C}_4\text{H}_{10}/\text{N}_2$ . As mentioned earlier, this behavior is unusual for conventional glassy polymers, which are typically size-selective (i.e., selective for the smaller nitrogen molecule over the larger hydrocarbons).<sup>28,29</sup> Table 3 also shows that selectivities generally increase as permeability and FFV decrease. That is, pure-gas selectivities increase in the order PTMSP ( $\text{FFV} \sim 0.29$ ) < PMP ( $\text{FFV} \sim 0.28$ ) ≤ PTMSDPA ( $\text{FFV} \sim 0.26$ ) < PPP ( $\text{FFV} \sim 0.22$ ). The

PMP  $\text{CH}_4/\text{N}_2$  and  $\text{C}_2\text{H}_6/\text{N}_2$  selectivities and the PPP  $n\text{-C}_4\text{H}_{10}/\text{N}_2$  selectivity, however, are exceptions to this trend.

The selectivity behavior observed as polymer FFV decreases may be rationalized based on the solution-diffusion mechanism used to describe gas transport through polymer films.<sup>30</sup> The permeability coefficient in eq 2 can be expressed as

$$P = DS \quad (6)$$

where  $D$  is the effective average diffusion coefficient ( $\text{cm}^2/\text{s}$ ) and  $S$  is the solubility coefficient [ $\text{cm}^3(\text{STP})/(\text{cm}^3\cdot\text{cmHg})$ ]. The selectivity defined in eq 3 can then be written as

$$\alpha_{A/B} = \frac{D_A}{D_B} \times \frac{S_A}{S_B} \quad (7)$$

where  $D_A/D_B$ , the ratio of the diffusion coefficients, is the mobility (diffusivity) selectivity and  $S_A/S_B$ , the ratio of the sorption coefficients, is the solubility selectivity. Therefore, selectivity is determined by the balance of the mobility and solubility selectivities in the polymer. Because penetrant mobility decreases with increasing penetrant size, diffusivity selectivity ( $D_A/D_B$ ) always favors the smaller permeant. For the separation of organic vapors from permanent gases,  $D_A/D_B$  is less than unity because the diffusion coefficient of the larger vapor molecule (A) is always less than that of the smaller permanent-gas molecule (B). On the other hand, the solubility selectivity ( $S_A/S_B$ ) favors the more condensable organic-vapor molecule because solubility usually increases with increasing molecular size (or increasing condensability). Hence,  $S_A/S_B$  is greater than unity for organic-vapor/permanent-gas separation. In traditional, low free volume, glassy polymers, diffusion coefficients decrease more with increasing penetrant size than solubility coefficients increase with increasing penetrant size. Consequently, in conventional glasses, gas permeabilities generally decrease with increasing penetrant size.<sup>28,30,31</sup>

According to eq 7, the selectivity trends observed in the disubstituted acetylene polymers can be rationalized by considering the solubility and mobility selectivity terms separately. The data in Table 3 can be divided into two groups: (i) gas/nitrogen selectivities, where "gas" refers to helium, hydrogen, oxygen, and carbon dioxide and (ii) hydrocarbon/nitrogen selectivities. For gas/nitrogen pairs, the kinetic diameters of helium (2.6 Å), hydrogen (2.89 Å), oxygen (3.46 Å), and carbon dioxide (3.3 Å) are smaller than that of nitrogen (3.64 Å).<sup>32</sup> Hence, the mobility selectivity ( $D_{\text{gas}}/D_{\text{N}_2}$ ) should be greater than unity for the  $\text{He}/\text{N}_2$ ,  $\text{H}_2/\text{N}_2$ ,  $\text{O}_2/\text{N}_2$ , and  $\text{CO}_2/\text{N}_2$  gas pairs. Because the chemical structures of PTMSP, PMP, PTMSDPA, and PPP are similar, the gas/nitrogen solubility selectivity ( $S_{\text{gas}}/S_{\text{N}_2}$ ) is not expected to be very different for these four disubstituted acetylene polymers. For example, at 25 °C, the  $\text{O}_2/\text{N}_2$  solubility selectivities of PTMSP and PPP are 1.2 and 1.7, respectively.<sup>12</sup> Therefore, the selectivity increase observed with decreasing polymer FFV probably results from diffusivity selectivity ( $D_{\text{gas}}/D_{\text{N}_2}$ ) becoming increasingly greater than unity. The ranking of ( $D_{\text{gas}}/D_{\text{N}_2}$ ) in the substituted acetylene polymers is expected to be PPP > PTMSDPA > PMP > PTMSP > 1, exactly opposite to the trend in FFV and in qualitative agreement with the Cohen–Turnbull theory of the effect of free

**Table 4. Comparison of Gas Permeabilities and Selectivities in Glassy Disubstituted Acetylene Polymers (PTMSP, PMP, PTMSDPA) and Conventional Glassy Polymers at 25 °C**

polymer	permeability (barrer) <sup>f</sup>			selectivity		
	N <sub>2</sub>	C <sub>3</sub> H <sub>8</sub>	<i>n</i> -C <sub>4</sub> H <sub>10</sub>	O <sub>2</sub> /N <sub>2</sub>	C <sub>3</sub> H <sub>8</sub> /H <sub>2</sub>	<i>n</i> -C <sub>4</sub> H <sub>10</sub> /H <sub>2</sub>
High Free Volume Polyacetylenes						
PTMSP	6300 <sup>a</sup>	32000	102000	1.5 <sup>a</sup>	1.9	6.0
PMP	1300 <sup>b</sup>	7300	26000	2.1 <sup>b</sup>	1.3	4.5
PTMSDPA	560	4400	20000	2.1	1.7	7.7
Low Free Volume Glassy Polymers						
PPP	21 <sup>c</sup>		52 <sup>c</sup>		2.7 <sup>c</sup>	0.19 <sup>c</sup>
polysulfone	0.24 <sup>d</sup>		0.16 <sup>e</sup>		5.8 <sup>d</sup>	0.015 <sup>d,e</sup>

<sup>a</sup> Reference 3. <sup>b</sup> Reference 9. <sup>c</sup> Reference 14. <sup>d</sup> Reference 26.

<sup>e</sup> *n*-C<sub>4</sub>H<sub>10</sub> permeability was obtained at 35 °C at a feed pressure of 744 mmHg and a permeate pressure of 0 mmHg in a 34 μm-thick polysulfone film. <sup>f</sup> 1 barrer = 10<sup>-10</sup> cm<sup>3</sup>(STP)·cm/(cm<sup>2</sup>·s·cmHg). Feed pressure = 50 psig (446 kPa), except for *n*-C<sub>4</sub>H<sub>10</sub> (8 psig (156 kPa) for PTMSP, PMP, and PTMSDPA; 16 psig (212 kPa) for PPP). Permeate pressure = 0 psig (101 kPa).

volume on diffusion coefficients.<sup>33</sup> In this model, diffusion coefficients decrease more strongly with increasing penetrant size in lower free volume environments.<sup>27,33</sup> Thus, for the He/N<sub>2</sub>, H<sub>2</sub>/N<sub>2</sub>, O<sub>2</sub>/N<sub>2</sub>, and CO<sub>2</sub>/N<sub>2</sub> pairs, gas/nitrogen selectivities in PTMSDPA should be higher than in PTMSP and PMP and lower than in PPP, consistent with the data in Table 3.

For hydrocarbon/nitrogen selectivities, the mobility selectivity ( $D_{\text{hydrocarbon}}/D_{\text{N}_2}$ ) is less than unity because the hydrocarbons are larger than nitrogen. On the basis of the average free volume in the polymer matrix, ( $D_{\text{hydrocarbon}}/D_{\text{N}_2}$ ) values are expected to be in the following order: 1 > PTMSP > PMP > PTMSDPA > PPP. If solubility selectivities of these polymers are similar, the overall selectivity should also be in the order of the diffusivity selectivities. On the basis of the data in Table 3, this is not the case. Unlike gases, such as hydrogen and nitrogen, the hydrocarbon penetrants are more condensable and may plasticize the polymer matrix. As a result, hydrocarbon permeabilities and, hence, hydrocarbon/nitrogen selectivities would be sensitive to the feed pressure of the measurements. For example, plasticization of PMP by propane and *n*-butane has been observed at 35 °C over a pressure range of 5–100 psig.<sup>9</sup> Because hydrocarbon/nitrogen selectivities do not increase monotonically with decreasing polymer FFV for all hydrocarbon penetrants in Table 3, this result may reflect the different feed-pressure dependencies of the hydrocarbon permeabilities in the various polyacetylenes. For example, the C<sub>3</sub>H<sub>8</sub>/N<sub>2</sub> and *n*-C<sub>4</sub>H<sub>10</sub>/N<sub>2</sub> selectivities in PTMSDPA and PMP are higher than those in PTMSP due, most probably, to greater plasticization of the PTMSDPA and PMP matrices by these higher hydrocarbons. The PPP *n*-C<sub>4</sub>H<sub>10</sub>/N<sub>2</sub> selectivity, though, is much lower than that in the other three polymers presumably because of its lower free volume and a weaker tendency for plasticization under the testing conditions. More detailed studies of the pressure dependence of the gas permeability coefficients in these polyacetylenes would be needed to completely address this issue.

Table 4 compares selected permeabilities and selectivities of PTMSDPA to those of PTMSP, PMP, PPP, and polysulfone. These permeabilities and selectivities were chosen because they pertain to industrially important gas separations, specifically, the separation of oxygen from nitrogen and of C<sub>3</sub>+ hydrocarbons from

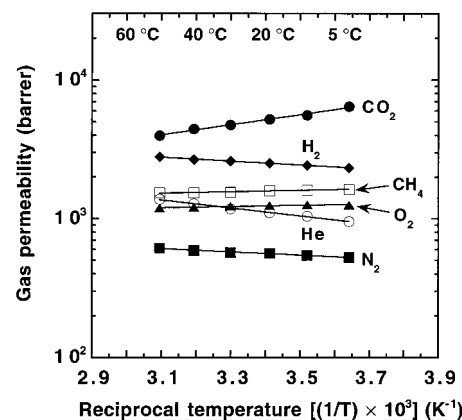


**Figure 3.** Arrhenius plot of various gas permeabilities in high free volume, glassy PTMSDPA as a function of reciprocal temperature ( $1/T$ ). Activation energies of permeation ( $E_p$ ) were calculated from the slopes of the best-fit lines. Feed pressure: 50 psig. Permeate pressure: 0 psig. [1 barrer = 10<sup>-10</sup> cm<sup>3</sup>(STP)·cm/(cm<sup>2</sup>·s·cmHg).]

hydrogen. Although its permeabilities are lower than those of PTMSP and PMP, PTMSDPA is a high-permeability material, more similar to PTMSP and PMP than to PPP or polysulfone. PTMSDPA, like PTMSP and PMP, possesses low permanent-gas (e.g., O<sub>2</sub>/N<sub>2</sub>) selectivities and is more permeable to hydrocarbon vapors (C<sub>3</sub>H<sub>8</sub>, *n*-C<sub>4</sub>H<sub>10</sub>) than to light gases, such as hydrogen. PPP, though, exhibits the opposite behavior and provides an interesting contrast to the hydrocarbon permeation properties of the other substituted acetylene polymers. PPP is about 5 times more permeable to hydrogen than to *n*-butane. Polysulfone is markedly more permeable to hydrogen than to *n*-butane and has an O<sub>2</sub>/N<sub>2</sub> selectivity 2–4 times higher than that of the polyacetylenes. These selectivity values are in accord with the much stronger size-sieving ability of polysulfone. The polysulfone permeability and selectivity values are qualitatively consistent with its substantially lower FFV (~0.16),<sup>14,21</sup> relative to that of the polyacetylenes.

**Effect of Temperature on Gas Permeability of PTMSDPA.** Gas permeabilities in PTMSDPA were determined over a temperature range of 1.5–50 °C. As shown in Figure 3, the permeabilities of nitrogen, helium, and hydrogen in PTMSDPA increase with increasing temperature. In contrast, methane, oxygen, and carbon dioxide permeabilities decrease with increasing temperature. While permeabilities generally increase with increasing temperature for conventional glassy polymers,<sup>30</sup> decreases in permeability with increasing temperature have been reported in high free volume, glassy PTMSP and PMP.<sup>9,12</sup>

The temperature dependence of gas permeability in polymers is given by the Arrhenius relationship<sup>30</sup>

$$P = P_0 \exp\left(-\frac{E_p}{RT}\right) \quad (8)$$

where  $P_0$  is a preexponential factor [cm<sup>3</sup>(STP)·cm/(cm<sup>2</sup>·s·cmHg)],  $E_p$  is the activation energy of permeation (J/mol),  $R$  is the gas constant [8.314 J/(mol·K)], and  $T$  is the temperature (K).  $E_p$  is determined from a plot of the logarithm of permeability ( $\ln P$ ) vs reciprocal temperature ( $1/T$ ).  $E_p$  values for PTMSDPA were estimated from the slopes ( $-E_p/R$ ) of the best-fit lines through the permeation data in Figure 3.

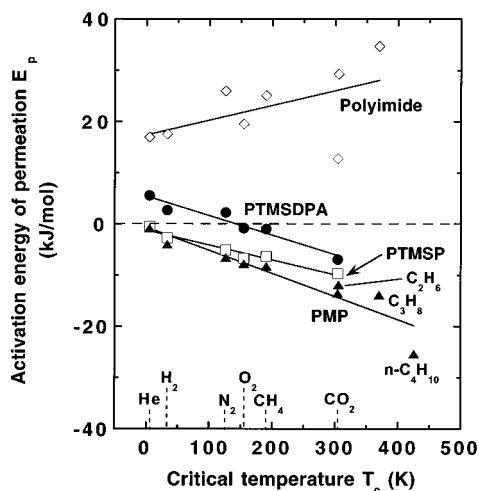


**Figure 4.** Comparison of activation energies of permeation ( $E_p$ ) for various penetrants in PTMSDPA (●) to activation energies in PTMSP<sup>12</sup> (□), PMP<sup>9</sup> (▲), and low free volume, glassy polyimide<sup>34</sup> (◇) as a function of penetrant critical temperature.<sup>38</sup>

Because  $P$  can be expressed as the product of diffusivity  $D$  and solubility  $S$  (eq 6), the activation energy of permeation  $E_p$  can be written as follows:<sup>30</sup>

$$E_p = E_d + \Delta H_s \quad (9)$$

where  $E_d$  is the activation energy of diffusion (J/mol) and  $\Delta H_s$  is the heat of sorption (J/mol). Because penetrant diffusion coefficients always increase with increasing temperature,  $E_d$  is positive.<sup>30,31</sup> Penetrant sorption is often an exothermic process, particularly in glassy polymers and for the more condensable, hydrocarbon penetrants. Hence,  $\Delta H_s$  is generally negative.<sup>31</sup> In conventional, low free volume, glassy polymers, the magnitude of  $E_d$  is usually greater than the absolute value of  $\Delta H_s$ . As a result,  $E_p$  is typically positive for all penetrants in conventional glassy polymers, and permeabilities increase with increasing temperature.<sup>30</sup>

However, as shown in Figure 4, in high free volume, glassy polymers such as PTMSP and PMP,  $E_p$  values are negative for all gases tested, indicating that gas permeability coefficients are higher at lower temperatures, which is an extremely unusual trend for glassy polymers.<sup>9,12</sup> Figure 4 also clearly demonstrates that  $E_p$  values for these two disubstituted acetylene polymers becomes more negative with increasing critical temperature  $T_c$  (condensability) of the penetrant. This behavior is contrasted in the same figure to the activation energy of permeation for a high-performance, relatively low free volume, glassy, aromatic polyimide.<sup>34</sup>  $E_p$  values for the polyimide are positive for all permeants and generally increase with increasing penetrant size. To date, negative  $E_p$  values in glassy polymers have been observed only for these very high free volume polyacetylenes, suggesting that the temperature dependence of gas permeation is controlled by the negative heats of sorption coupled with a very weak size-sieving ability, which leads to very low activation energies of diffusion.<sup>9,12</sup>

Activation energies of permeation in PTMSDPA are also presented in Figure 4. Because the activation energy of permeation decreases with increasing penetrant critical temperature, the  $E_p$  behavior for PTMSDPA is similar to that of high free volume PTMSP and PMP. However, in contrast to PTMSP and PMP, PTMSDPA exhibits negative  $E_p$  values only for pen-

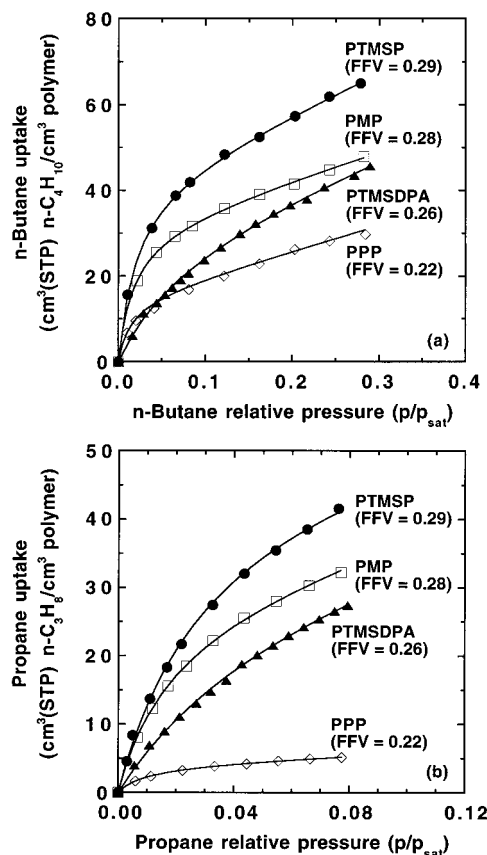


**Figure 5.** Comparison of (a) *n*-butane and (b) propane sorption isotherms for PMP at 35 °C and PTMSDPA at 36 °C to those reported for PTMSP<sup>20</sup> and PPP<sup>20</sup> at 35 °C. Solid curves are dual-mode fits to the data. Dual-mode parameters are given in Table 5. Saturation vapor pressure ( $p_{\text{sat}}$ ): 2469.5 mmHg at 35 °C and 2541.7 mmHg at 36 °C for *n*-butane; 9151.7 mmHg at 35 °C and 9371.4 mmHg at 36 °C for propane.<sup>38</sup> (FFV = fractional free volume of polymer).

etrants with  $T_c > 130$  K and exhibits positive  $E_p$  for gases with lower critical temperatures.

***n*-Butane and Propane Sorption in Polyacetylenes.** The *n*-butane and propane sorption isotherms of PTMSDPA and PMP are compared to those reported for PTMSP<sup>20</sup> and PPP<sup>20</sup> in parts a and b of Figure 5. Hydrocarbon uptake in PTMSDPA and PMP increases with increasing penetrant relative pressure. *n*-Butane and propane sorption levels at fixed relative pressure decrease in the order PTMSP > PMP > PTMSDPA > PPP. Penetrant uptake is significantly lower in PTMSDPA and PMP than in PTMSP. For example, at a *n*-butane relative pressure of 0.3, PMP sorbs 48 cm<sup>3</sup>(STP) *n*-C<sub>4</sub>H<sub>10</sub>/cm<sup>3</sup> PMP (~16% of its own weight in *n*-butane). PTMSDPA takes up 46 cm<sup>3</sup>(STP) *n*-C<sub>4</sub>H<sub>10</sub>/cm<sup>3</sup> PTMSDPA (~13% of its own weight in *n*-butane). PTMSP, however, sorbs 65 cm<sup>3</sup>(STP) *n*-C<sub>4</sub>H<sub>10</sub>/cm<sup>3</sup> PTMSP, which corresponds to 22% of its own weight in *n*-butane, at the same relative pressure. Likewise, at a relative pressure of 0.08, the propane sorption level is 33 cm<sup>3</sup>(STP)/cm<sup>3</sup> (~8.3 wt %) in PMP and 27 cm<sup>3</sup>(STP)/cm<sup>3</sup> (~5.8 wt %) in PTMSDPA. These levels are much lower than that of PTMSP, which sorbs about 41 cm<sup>3</sup>(STP)/cm<sup>3</sup> (~11 wt %) of propane. On the other hand, the hydrocarbon sorption levels in PTMSDPA and PMP are substantially higher than those in PPP. At the same relative pressures given above, PPP sorbs only 30 cm<sup>3</sup>(STP)/cm<sup>3</sup> (~7.8 wt %) of *n*-butane and 5.1 cm<sup>3</sup>(STP)/cm<sup>3</sup> (~1.0 wt %) of propane. The order of the



sorption levels in these polyacetylenes is consistent with the ranking of their FFV values.

The concavity of the sorption isotherms with respect to the relative pressure axis at low pressure is the signature of so-called dual-mode behavior. The dual-mode model of penetrant sorption is used to describe such isotherms in glassy materials at low to moderate penetrant pressures.<sup>30</sup> According to dual-mode theory, penetrant molecules partition into two types of sorption sites in the glassy polymer, and these sites are in dynamic equilibrium. Penetrant molecules sorb into the equilibrium, densified regions of the polymer matrix according to Henry's law and into the unrelaxed, molecular-scale gaps (microvoids) frozen into the glassy state according to a Langmuir isotherm.<sup>30</sup> Because the Langmuir contribution arises from the inherently non-equilibrium nature of the glassy state, it accounts for sorption into the nonequilibrium excess free volume of the material. In terms of penetrant relative pressure  $a$  [i.e.,  $p/p_{\text{sat}}$ ], the dual-mode sorption model is given by the algebraic sum of the two contributions to penetrant concentration  $C$  [ $\text{cm}^3(\text{STP})$  penetrant/ $\text{cm}^3$  polymer]:<sup>30</sup>

$$C = k_D a + \frac{C_H b a}{1 + b a} \quad (10)$$

where  $k_D$  is the Henry's law coefficient [ $\text{cm}^3(\text{STP})$  penetrant/ $\text{cm}^3$  polymer],  $b$  is the Langmuir affinity parameter (dimensionless), and  $C_H$  is the Langmuir capacity parameter [ $\text{cm}^3(\text{STP})$  penetrant/ $\text{cm}^3$  polymer]. The Henry's law coefficient  $k_D$  represents the equilibrium partition coefficient of penetrant dissolved in the polymer matrix. The Langmuir affinity parameter  $b$  characterizes the tendency of a penetrant to sorb into a Langmuir site. The Langmuir capacity parameter  $C_H$  is a measure of the maximum sorption capacity of the Langmuir domains. The  $C_H$  value is often related to the nonequilibrium excess free volume ( $\hat{V}_g - \hat{V}_l$ ) in a glassy polymer by<sup>30,35,36</sup>

$$C_H = 22\,414 \left( \frac{\hat{V}_g - \hat{V}_l}{\hat{V}_g} \right) \rho^* \quad (11)$$

where  $\hat{V}_g$  and  $\hat{V}_l$  are the polymer specific volumes ( $\text{cm}^3/\text{g}$ ) in the glassy and hypothetical rubbery states and  $\rho^*$  is the molar density ( $\text{mol}/\text{cm}^3$ ) of penetrant as it exists in the Langmuir sites. For penetrants, such as  $n$ -butane and propane, which are below their critical temperatures,  $\rho^*$  is often set to the liquid (condensed) density of pure penetrant at the temperature of the experiment.<sup>30,36</sup> The nonequilibrium excess free volume fraction in a glassy polymer is given by the ratio  $[C_H/(22414\rho^*)]$ .

Dual-mode parameters obtained from a nonlinear least-squares regression analysis of the hydrocarbon sorption data (Figure 5) are summarized in Table 5. For the  $n$ -butane sorption data, the regression analysis was performed with all dual-mode parameters treated as adjustable constants. PTMSDPA and PMP have comparable  $k_D$  and  $C_H$  values, which are 25–30% and 16–30% lower, respectively, than those in PTMSP. Compared to the  $k_D$  and  $C_H$  values for PPP, however, the  $k_D$  and  $C_H$  values of PTMSDPA and PMP are higher. The  $b$  values of PTMSDPA and PMP are 12 and 56, respectively. While there is no obvious, definitive trend in the  $k_D$  or  $b$  values with polymer structure, it is interesting that the TMS-containing polymers, PTMSP

**Table 5. Dual-Mode Parameters for  $n$ -Butane ( $n\text{-C}_4\text{H}_{10}$ ) and Propane ( $\text{C}_3\text{H}_8$ ) Sorption in PTMSP, PMP, PTMSDPA, and PPP at 35 °C**

penetrant	polymer	dual-mode parameters <sup>a</sup>		
		$k_D$ ( $\text{cm}^3(\text{STP})$ penetrant/ $\text{cm}^3$ of polymer)	$C_H$ ( $\text{cm}^3(\text{STP})$ penetrant/ $\text{cm}^3$ of polymer)	$b$
$n\text{-C}_4\text{H}_{10}$	PTMSP <sup>b</sup>	90	43	48
	PMP	62	32	56
	PTMSDPA <sup>c</sup>	76	30	12
	PPP <sup>f</sup>	58	15	70
$\text{C}_3\text{H}_8$	PTMSP <sup>b</sup>	69 (fixed)	50	30
	PMP <sup>d</sup>	66	36 (fixed)	39
	PTMSDPA <sup>c,e</sup>	100	34 (fixed)	17
	PPP <sup>f</sup>	21	4.0	100

<sup>a</sup> Units based on penetrant relative pressure  $a = p/p_{\text{sat}}$ . <sup>b</sup> Reference 20; dual-mode fit performed at fixed  $k_D$  for  $\text{C}_3\text{H}_8$  sorption data. <sup>c</sup>  $T = 36$  °C. <sup>d</sup> On the basis of an analysis with  $C_H$  fixed at the given value such that  $[C_H/(22414\rho^*)] = 0.15$ . <sup>e</sup> On the basis of an analysis with  $C_H$  fixed at the given value such that  $[C_H/(22414\rho^*)] = 0.14$ . <sup>f</sup> Reference 20.

and PTMSDPA, have higher  $k_D$  and lower  $b$  values than the purely hydrocarbon-based polyacetylenes, PMP and PPP.

For the propane data, however, the regression analysis was performed with a fixed  $C_H$  value. This two-parameter fit was conducted because of the difficulty in determining unique dual-mode parameters for the propane data obtained over the limited relative pressure range 0–0.08. Regardless of whether one parameter is fixed or all parameters are treated as adjustable, the experimental propane data could be well-described by different sets of dual-mode parameters. This drawback of the empirical dual-mode model has been previously reported.<sup>20</sup> The resolution and reliability of the dual-mode fit improve if a wider relative pressure range is explored to provide a larger fraction of the complete sorption isotherm.<sup>20</sup> Because the  $n$ -butane sorption isotherms investigate a wider relative pressure range due to a lower  $n$ -butane saturation vapor pressure, the  $n$ -butane dual-mode parameters should be less dependent on the pressure range of the measurement. Thus, it seems reasonable to fix the propane  $C_H$  value such that the excess free volume fraction  $[C_H/(22414\rho^*)]$  estimated from the propane data is equal to that computed from  $n$ -butane sorption data. Morisato et al. have shown that, for PTMSP, excess free volume fractions determined from the sorption of penetrants having different size and chemical nature under different experimental conditions are quite similar.<sup>20</sup> In particular, the  $[C_H/(22414\rho^*)]$  values obtained from propane and  $n$ -butane sorption data for PTMSP are essentially the same.<sup>20</sup> The propane dual-mode parameters resulting from the two-parameter analysis are recorded in Table 5.

As the FFV of a polymer decreases, the Langmuir sorption capacity can be expected to be smaller. This trend is seen on the order of  $n$ -butane  $C_H$  values relative to the ranking of the FFVs. As summarized in Table 6, the nonequilibrium excess free volume fraction based on  $n$ -butane sorption data is 0.14 for PTMSDPA and 0.15 for PMP. These values, though similar, indicate that PTMSDPA may have a slightly lower excess free volume than PMP. Compared to PTMSP (excess free volume fraction  $\approx 0.20$ – $0.21$ ), PTMSDPA and PMP have significantly lower excess free volume fractions. The smaller excess free volumes in PTMSDPA and PMP

**Table 6. Nonequilibrium Excess Free Volume Fraction Estimated from Propane ( $C_3H_8$ ) and *n*-Butane ( $n-C_4H_{10}$ ) Sorption Data at 35 °C for PTMSP, PMP, PTMSDPA, and PPP**

polymer	excess free volume fraction $[(C_H/22414\rho^*)]^c$	
	$C_3H_8$	$n-C_4H_{10}$
PTMSP <sup>a</sup>	0.21	0.20
PMP	0.15 (fixed)	0.15
PTMSDPA <sup>b</sup>	0.14 (fixed)	0.14
PPP <sup>a</sup>	0.02	0.07

<sup>a</sup> On the basis of the  $C_H$  value reported in ref 20. <sup>b</sup>  $T = 36$  °C. <sup>c</sup>  $M\rho^* = 0.476$  g/cm<sup>3</sup> at 35 °C and 0.474 g/cm<sup>3</sup> at 36 °C for  $C_3H_8$  and 0.561 g/cm<sup>3</sup> at 35 °C and 0.560 g/cm<sup>3</sup> at 36 °C for  $n-C_4H_{10}$ ,<sup>38</sup> where  $M$  is penetrant molecular weight.

are consistent with their lower FFV values. Nevertheless, the excess free volumes in PMP and PTMSDPA are very high, compared to an excess free volume of only 2–7% in PPP<sup>20</sup> and 3–9% in conventional glassy polymers.<sup>8,37</sup>

Within the framework of the dual-mode theory, the overall hydrocarbon sorption is lower in PTMSDPA and PMP than in PTMSP due primarily to lower sorption levels in the Langmuir sites. The reduced sorption levels in the nonequilibrium excess free volume of PTMSDPA and PMP are related to the lower FFV values in these polymers, relative to that in PTMSP. A similar line of reasoning explains the much lower hydrocarbon uptake in PPP, compared to that of the other polyacetylenes. In PTMSDPA, the decrease in Langmuir sorption at a given relative pressure is also related to its lower Langmuir affinity parameter ( $b$ ) value, implying that penetrant molecules have a reduced tendency to sorb into the microvoid domains frozen into this glassy material.

## Conclusions

Like poly(1-trimethylsilyl-1-propyne) [PTMSP] and poly(4-methyl-2-pentyne) [PMP], poly[1-phenyl-2-[*p*-(trimethylsilyl)phenyl]acetylene] [PTMSDPA] is more permeable to large hydrocarbons (e.g., propane and *n*-butane) than to smaller, permanent gases (e.g., nitrogen and hydrogen). This vapor-selective behavior of PTMSDPA differs from that of poly(1-phenyl-1-propyne) [PPP], which is gas-selective and one of the least permeable disubstituted acetylene polymers. Fractional free volume (FFV) and gas permeability of these materials decrease in the order PTMSP > PMP > PTMSDPA > PPP. As temperature increases, the permeability in PTMSDPA increases for permanent gases [positive activation energies of permeation ( $E_p$ )] and decreases for larger, more condensable gases [negative  $E_p$ ]. This behavior is different from that reported for PTMSP and PMP, which have negative  $E_p$  values for all gases, and atypical of conventional glasses, which have positive  $E_p$  values. The temperature dependence of permeability in PTMSDPA suggests that PTMSDPA may be a borderline material between high free volume, glassy polyacetylenes and common, low free volume, glassy polymers. *n*-Butane and propane sorption levels in PTMSDPA, PMP, and PPP are lower than those in PTMSP due primarily to lower amounts of nonequilibrium excess free volume in these three polymers.

**Acknowledgment.** The authors gratefully acknowledge support of this work by the Department of Energy through the Small Business Innovation Research Pro-

gram (Grant DE-FG03-94ER81811) and the National Science Foundation [CTS-9803225]. The research described in this publication was made possible in part by Award No RC2-347 of the U.S. Civilian Research and Development Foundation for the Independent States of the Former Soviet Union (CRDF).

## References and Notes

- (1) Toy, L. G.; Pinnau, I.; Baker, R. W. *U.S.* 5,281,255 1994.
- (2) Pinnau, I.; Casillas, C. G.; Morisato, A.; Freeman, B. D. *J. Polym. Sci., Part B: Polym. Phys.* **1996**, *34*, 2613–2621.
- (3) Pinnau, I.; Toy, L. G. *J. Membr. Sci.* **1996**, *116*, 199–209.
- (4) Freeman, B. D.; Pinnau, I. In *Polymer Membranes for Gas and Vapor Separation: Chemistry and Materials Science*; Freeman, B. D., Pinnau, I., Eds.; ACS Symposium Series 733; American Chemical Society: Washington, DC, 1999; pp 1–27.
- (5) Masuda, T.; Isobe, E.; Higashimura, T.; Takada, K. *J. Am. Chem. Soc.* **1983**, *105*, 7473–7474.
- (6) Merkel, T. C.; Bondar, V.; Nagai, K.; Freeman, B. D. *J. Polym. Sci., Part B: Polym. Phys.* **2000**, *38*, 273–296.
- (7) Merkel, T. C.; Bondar, V.; Nagai, K.; Freeman, B. D. *Macromolecules* **1999**, *32*, 370–374.
- (8) Srinivasan, R.; Auvil, S. R.; Burban, P. M. *J. Membr. Sci.* **1994**, *86*, 67–86.
- (9) Morisato, A.; Pinnau, I. *J. Membr. Sci.* **1996**, *121*, 243–250.
- (10) Masuda, T.; Kawasaki, M.; Okano, Y.; Higashimura, T. *Polym. J.* **1982**, *14*, 371–377.
- (11) Masuda, T.; Higashimura, T. *Adv. Polym. Sci.* **1987**, *81*, 121–165.
- (12) Masuda, T.; Iguchi, Y.; Tang, B.-Z.; Higashimura, T. *Polymer* **1988**, *29*, 2041–2049.
- (13) Odani, H.; Masuda, T. In *Polymers for Gas Separation*; Toshima, N., Ed.; VCH Publishers: New York, NY, 1992; pp 107–144.
- (14) Morisato, A.; Shen, H. C.; Sankar, S. S.; Freeman, B. D.; Pinnau, I.; Casillas, C. G. *J. Polym. Sci., Part B: Polym. Phys.* **1996**, *34*, 2209–2222.
- (15) Teraguchi, M.; Masuda, T. *J. Polym. Sci., Part A: Polym. Chem.* **1998**, *36*, 2721–2725.
- (16) Tsuchihara, K.; Masuda, T.; Higashimura, T. *J. Am. Chem. Soc.* **1991**, *113*, 8548–8549.
- (17) Tsuchihara, K.; Masuda, T.; Higashimura, T. *Macromolecules* **1992**, *25*, 5816–5820.
- (18) Stern, S. A.; Gareis, P. J.; Sinclair, T. F.; Mohr, P. H. *J. Appl. Polym. Sci.* **1963**, *7*, 2035–2051.
- (19) Ichiraku, I.; Stern, S. A.; Nakagawa, T. *J. Membr. Sci.* **1987**, *34*, 5–18.
- (20) Morisato, A.; Freeman, B. D.; Pinnau, I.; Casillas, C. G. *J. Polym. Sci., Part B: Polym. Phys.* **1996**, *34*, 1925–1934.
- (21) Pixon, M. R.; Paul, D. R. In *Polymeric Gas Separation Membranes*; Paul, D. R., Yampol'skii, Y. P., Eds.; CRC Press: Boca Raton, FL, 1994; pp 83–153.
- (22) Lee, W. M. *Polym. Eng. Sci.* **1980**, *20* (1), 65–69.
- (23) van Krevelen, D. W. *Properties of Polymers: Their Correlation with Chemical Structure; Their Numerical Estimation and Prediction from Additive Group Contributions*, 3rd ed.; Elsevier Science: Amsterdam, 1990; pp 71–107.
- (24) Bondi, A. *Physical Properties of Molecular Crystals, Liquids, and Glasses*; John Wiley and Sons: New York, 1968; pp 25–52, 53–97.
- (25) Nakagawa, T. In *Science and Technology of Polymers and Advanced Materials: Emerging Technologies and Business Opportunities*; Prasad, P. N., Mark, J. E., Kandil, S. H., Kafafi, Z. H., Eds.; Plenum Press: New York, 1998; pp 821–834.
- (26) *Permeability and Other Film Properties*; Plastics Design Library: New York, 1995; 283–285.
- (27) Freeman, B. D.; Hill, A. J. In *Structures and Properties of Glassy Polymers*; Tant, M. R., Hill, A. J., Eds.; ACS Symposium Series 710; American Chemical Society: Washington, DC, 1998; pp 306–325.
- (28) Baker, R. W.; Wijmans, J. G. In *Polymeric Gas Separation Membranes*; Paul, D. R., Yampol'skii, Y. P., Eds.; CRC Press: Boca Raton, FL, 1994; 353–397.
- (29) Freeman, B.; Pinnau, I. *Trends Polym. Sci.* **1997**, *5* (5), 167–173.
- (30) Ghosal, K.; Freeman, B. D. *Polym. Adv. Technol.* **1994**, *5*, 673–697.
- (31) Koros, W. J.; Fleming, G. K. *J. Membr. Sci.* **1993**, *83*, 1–80.



- (32) Breck, D. W. *Zeolite Molecular Sieves: Structure, Chemistry, and Use*; John Wiley and Sons: New York, 1974; pp 593–724.
- (33) Cohen, M. H.; Turnbull, D. *J. Chem. Phys.* **1959**, *31*, 1164–1169.
- (34) Haraya, K.; Obata, K.; Hakuta, T.; Yoshitome, H. *Maku (Membrane)* **1986**, *11* (1), 48–52.
- (35) Koros, W. J.; Paul, D. R. *J. Polym. Sci., Polym. Phys. Ed.* **1978**, *16*, 1947–1963.
- (36) Chan, A. H.; Koros, W. J.; Paul, D. R. *J. Membr. Sci.* **1978**, *3*, 117–130.
- (37) Pinnau, I.; Casillas, C. G.; Morisato, A.; Freeman, B. D. *J. Polym. Sci., Polym. Phys. Ed.* **1997**, *35*, 1483–1490.
- (38) Reid, R. C.; Prausnitz, J. M.; Poling, B. E. *The Properties of Gases and Liquids*, 4th ed.; McGraw-Hill: New York, 1987; pp 29–73, 656–732.

MA991566E